



Composition, structure, magnetic and luminescent properties of EuFeO₃/TiO₂/Ti composites fabricated by combination of plasma electrolytic oxidation and extraction pyrolysis



V.S. Rudnev^{a, b, *}, N.I. Steblevskaya^a, K.N. Kilin^a, M.A. Medkov^a, I.A. Tkachenko^a, M.V. Belobeletskaya^a, M.V. Adigamova^a, I.V. Lukiyanchuk^a, P.M. Nedozorov^a, K.I. Yanushkevich^c

^a Institute of Chemistry, Far-Eastern Branch, Russian Academy of Sciences, 159, Prosp. 100-letya Vladivostoka, Vladivostok 690022, Russia

^b Far-Eastern Federal University, 8, Sukhanova Str., Vladivostok 690950, Russia

^c Scientific-Practical Materials Research Centre of the Belarus National Academy of Sciences, 17, P. Brovki Str., Minsk 22072, Belarus

ARTICLE INFO

Article history:

Received 27 February 2015

Received in revised form

20 May 2015

Accepted 22 June 2015

Available online 23 June 2015

Keywords:

EuFeO₃/TiO₂/Ti composites

Magnetic measurements

Luminescence

ABSTRACT

Layered oxide coatings containing europium ferrite multiferroic have been synthesized on titanium plates. With the presence of EuFeO₃, the composite acquires weak ferromagnetic properties: the coercive force attains 45–78 Oe in the temperature range 3–340 K. The magnetic properties of EuFeO₃/TiO₂/Ti composites are different from those of nanosized EuFeO₃ powder obtained by extraction pyrolysis. It has been established that EuFeO₃/TiO₂/Ti composites have luminescence properties characteristic of inorganic materials with europium ions. The obtained data assume that the deposited layer containing EuFeO₃ can have a complex structure: both oxidized and reduced elements may be present in its composition.

© 2015 Elsevier B.V. All rights reserved.

1. Introduction

A significant attention has been devoted recently to fabrication and study of ferroelectromagnetics (multiferroics) [1–11]. Multiferroics are substances characterized by at least two of three types of ordering: 1 – ferromagnetic (antiferromagnetic); 2 – ferroelectric; 3 – ferroelastic [1–4]. Based on these materials, one can create magnetic field sensors, electrically switched permanent magnets, magnetic memory cells, and other devices [2]. Aside from the thoroughly studied bismuth ferrite BiFeO₃ [1–3,6,8,9], this class of materials includes double ferrites of bismuth and rare earth elements (REE) [6,7] as well as REE ferrites, such as europium ferrites (EuFeO₃ and Eu₃Fe₅O₁₂) [10,11]. The interest to REE ferrites has grown considerably in recent years because of a wide range of catalytic, electrochemical, and optical properties characteristic for these compounds [12,13].

EuFeO₃ powders consisting of particles of a size of 10–20 nm were obtained using the extraction–pyrolysis method [11]. They are characterized by a complex behavior of the magnetization value. Up to ~230 K, the samples have low magnetization that increases dramatically at high temperatures. As early as at 300 K, the measured coercive force attained the value of 2068 Oe.

The extraction–pyrolysis (EP) method consisting in deposition of extracts of organic compounds containing the elements of interest at the preset stoichiometric ratio with subsequent annealing provides the possibility of both obtaining specific chemical compounds as powders and bulk samples and putting them on the surface of various substrates as separate areas or solid coatings [14]. When EP layers are deposited on metal substrate, its melting temperature must be higher than annealing temperature. To ensure good adhesion between the EP-layer and the metal substrate, sometimes it is necessary to create porous oxide layers on the metal substrate surface in advance [15,16]. Such porous oxide layers of a thickness from a few up to dozens of microns can be formed on valve metals (Al, Ti, Mg, etc.) by plasma electrolytic oxidation (PEO) technique comprising anodic or alternating current anode–cathode electrochemical oxidation of metal or alloy surface under spark and arc electric discharges in the near–anode area [17–19].

* Corresponding author. Institute of Chemistry, Far-Eastern Branch, Russian Academy of Sciences, 159, Prosp. 100-letya Vladivostoka, Vladivostok 690022, Russia.

E-mail address: rudnevvs@ich.dvo.ru (V.S. Rudnev).

It can be expected that the deposition of extracts proposed in Ref. [11] on the oxide PEO-coating followed by pyrolysis enables one to embed and fix EuFeO_3 multiferroic on metal substrate. Such composites can both have the properties inherent multiferroics and be promising as catalytically or optically active materials. It is of scientific interest to explore the possibility of application of combining the PEO and EP methods for forming such composites and to establish their structure, magnetic, and optical properties. Europium compounds are generally known luminophores [20–24]. The luminescent properties of europium ferrites are still studied insufficiently.

Since the pyrolysis of extract according to procedure of [11] is carried out at a temperature of 600 °C, and refractory valve metals such as titanium, zirconium or tantalum coated by appropriate oxides can be used as metal substrates. Note that combining the PEO and EP methods the 'EP-layer/PEO-coating/Ti' layered composites with protective or catalytic properties were obtained earlier [15,16].

The objective of the present work was to obtain $\text{EuFeO}_3/\text{TiO}_2/\text{Ti}$ composites using the methods of plasma electrolytic oxidation and extraction–pyrolysis synthesis and to study their composition, structure, and magnetic and luminescence properties.

2. Materials and methods

2.1. PEO coatings manufacturing

Layered coatings were deposited on plates made of titanium of the technical grade (VT1–0, 99.2–99.7 % Ti) of a size of $1.5 \times 0.5 \times 0.1 \text{ cm}^3$. The substrate pretreatment included chemical polishing in a mixture of concentrated acids $\text{HNO}_3:\text{HF} = 3:1$ (volume ratio) at ~343 K, washing with distilled water, and drying at ~340 K in air. Titanium-based anodic coatings were formed in the galvanostatic mode at an effective current density of 5 A/dm² for 10 min. The electrochemical cell comprised a vessel of a volume of 1 L made of thermally resistant glass with the anode-polarized treated sample, cathode in the form of a hollow coil made of nickel alloy, and thermometer placed inside. A computer-controlled TER4-100/460N thyristor device (Russia) working in the unipolar mode served as the current source. In the PEO coatings formation, the aqueous electrolyte of the following composition (mol/L) was used: 0.066 Na_3PO_4 + 0.034 $\text{Na}_2\text{B}_4\text{O}_7$ + 0.006 Na_2WO_4 (PBW electrolyte [25]). The electrolyte solution was stirred using a magnetic stirrer; it was cooled by passing cold tap water through the coil. The electrolyte temperature during the PEO process did not exceed 303 K.

2.2. Deposition of EuFeO_3 by extraction-pyrolysis method

The extraction–pyrolysis method of europium and iron oxides-based coatings deposition on TiO_2/Ti substrates was implemented in the following sequence: extraction of europium or iron from aqueous solution to obtain europium- and iron-saturated organic phases; mixing of saturated organic phases; solvent distillation to obtain the paste; paste deposition on the substrate with subsequent drying; finally, thermal decomposition of the obtained precursor to yield the oxide coating. It was established that to obtain saturated extracts for subsequent synthesis of multiferroics based on mixed europium and iron oxides using the pyrolysis method, one could successfully apply metal extraction by neutral, anion-exchange, and chelating extractants from chloride solutions [11]. To obtain saturated europium extracts, the chloride solution containing $6.6 \cdot 10^{-3} \text{ mol/L}$ of Eu^{3+} was used. The extraction was carried out by a mixture of 1.95 mol/L of acetylacetonate and 0.15 mol/L of phenanthroline in benzene. To obtain saturated

iron extracts, the iron chloride solution containing $3.6 \cdot 10^{-2} \text{ mol/L}$ Fe^{3+} and 1 mol/L HCl was used. In this case, the extraction was carried out by the benzene solution of 0.23 mol/L of tri-*n*-octylamine. In both cases, the phase ratio was 1:1, the stirring time was 30 min, whereas aqueous solutions were put three times in contact with the same organic phase. The compositions of aqueous solutions and organic phases were controlled using the atomic absorption and X-ray radiometric analysis as well as by luminescence and IR spectroscopy methods. The saturated solutions contained 0.011 mol/L Eu^{3+} and 0.07 mol/L Fe^{3+} . To obtain the precursor, organic solutions of europium (III) and iron (III) were mixed at the ratio $\text{Eu}:\text{Fe} = 1:1$, and the paste obtained upon the solvent distillation was deposited on the TiO_2/Ti substrate with alternating deposition and drying until the formation of a homogeneous layer. The TiO_2/Ti substrate with the deposited precursor was annealed in air in a PM–1–M muffle furnace (Russia) at 600 °C for 1 h. The time of furnace heating up to the working temperature was 40 min. The samples were taken out after the muffle furnace cooling. Pyrolysis of organic extracts with formation of europium ferrite took place as a result of annealing.

2.3. Composites characterization

The thickness of the coatings was determined using an Olympus LEXT OLS3100 confocal laser scanning microscope on their specially prepared chips.

To characterize the coatings we used X-ray spectrum (microprobe) analysis (XSA), scanning electron microscopy (SEM), energy dispersive X-ray analysis (EDXA), and X-ray diffraction (XRD).

The element composition, maps of elements distribution, and coatings surface features have been studied using a JEOL JXA 8100 electron probe micro-analyzer (Japan) supplemented with an INCA energy dispersive X-ray Spectrometer (Oxford Instruments, United Kingdom) (hereinafter referred to as XSA). The averaged element composition was determined from the results of scanning five surface areas of a size of $\sim 300 \times 300 \mu\text{m}^2$. Carbon was sputtered on the coatings surfaces prior to measurements.

The coating surface was also analyzed using a Hitachi S5500 high resolution electron microscope (Japan). In this case, we obtain SEM images of high resolution. Using a Thermo Scientific NSS spectral imaging system (USA) for energy dispersive analysis (hereinafter referred to as EDXA), we determined the element composition of some specific coating parts. Gold was preliminarily sputtered on coatings to prevent the surface charging.

The X-ray diffraction analysis (XRD) was carried out in $\text{CuK}\alpha$ radiation on a D8 ADVANCE X-ray diffractometer (Bruker, Germany). The EVA search program with the PDF–2 database was used in X-ray patterns processing.

2.4. Magnetic and luminescent properties

The composites magnetic properties were investigated on an SQUID MPMS 7 (Germany) magnetometer at temperatures from 3 K up to 340 K. The samples were magnetized in parallel to the magnetic field direction. In the magnetization calculations, the measured magnetic moment was normalized on the mass of the sample with coating. The coatings mass fractions were ~1–3 % from that of $\text{EuFeO}_3/\text{TiO}_2/\text{Ti}$ composites.

Luminescence excitation and emission spectra were recorded at 300 K using a Shimadzu RF-5000 spectrofluorimeter.

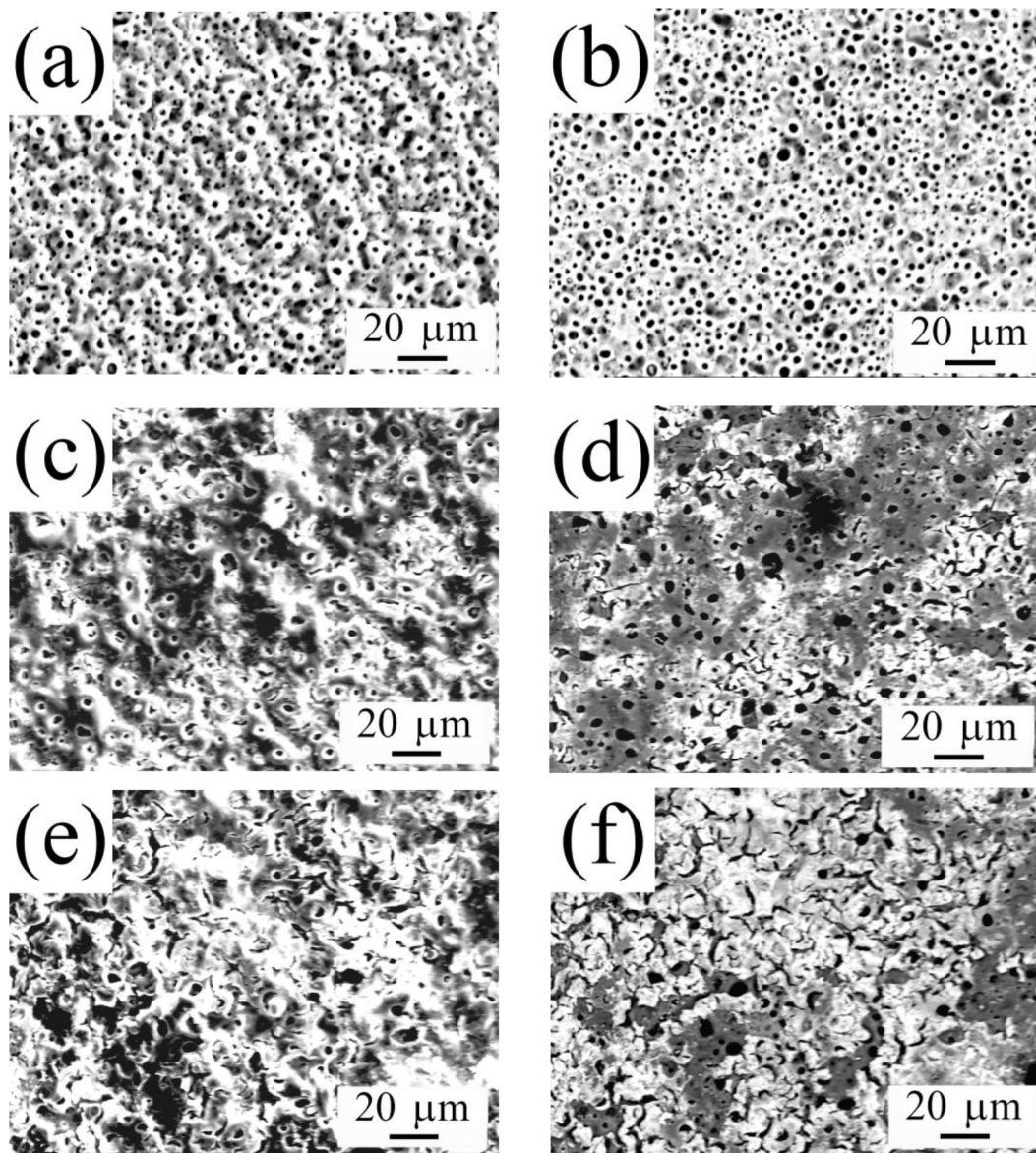


Fig. 1. SEM images of the PEO coating surface before (a, b) and after threefold (c, d) and fivefold (e, f) extract deposition with subsequent annealing. Amplitude (a, c, e) and phase (b, d, f) representation.

3. Results

3.1. The thickness, surface morphology, element and phase composition of the $\text{EuFeO}_3/\text{TiO}_2/\text{Ti}$ composites

The thickness of PEO coatings was $21 \pm 2 \mu\text{m}$. Within the measurement errors, the coating thickness did not change after their modification.

Fig. 1 shows SEM images of the surface of coatings on titanium obtained in the PBW electrolyte before (ab) and after threefold (cd) and fivefold (ef) extract deposition with subsequent annealing. Modification results in, first, formation of individual areas of the new phase on the surface (threefold deposition, Fig. 1cd) and, second, filling of larger surface areas (fivefold deposition, Fig. 1ef). The increase of the number of deposition cycles must allow formation of a solid layer of the new phase on the basic oxide coating surface. Initially (threefold deposition, Fig. 1cd), the new phase is attached predominantly in areas with larger quantities of small

pores, most probably, the surface sites having the largest defects. Thus, the oxide layer surface sorbs the extract selectively. Further deposition cycles (fivefold, Fig. 1ef) results in as in emergence of new areas of this type as in growth of the earlier formed ones.

The maps of elements distribution over the surface demonstrate that the new phase areas contain both europium and iron (Fig. 2), while the titanium contents in them are reduced. It is evident from comparison of Fig. 2b, c, and d that the titanium content is clearly lower in the sites of europium and iron localization than in neighboring areas. In other words, the PEO coating surface is closed (shielded) by a layer of the new phase. Since one detects titanium in the deposited areas and the analysis depth varies, depending to the nature of the analyzed material, from 2 to 5 μm , the thickness of the deposited modifying layer will be less than 2–5 μm . Here, the modifying layer heterogeneously shields the PEO coating surface. Aside from the areas that shield almost completely the initial coating, one also observes those with a partial shielding, as seen from the titanium distribution maps (Fig. 2).

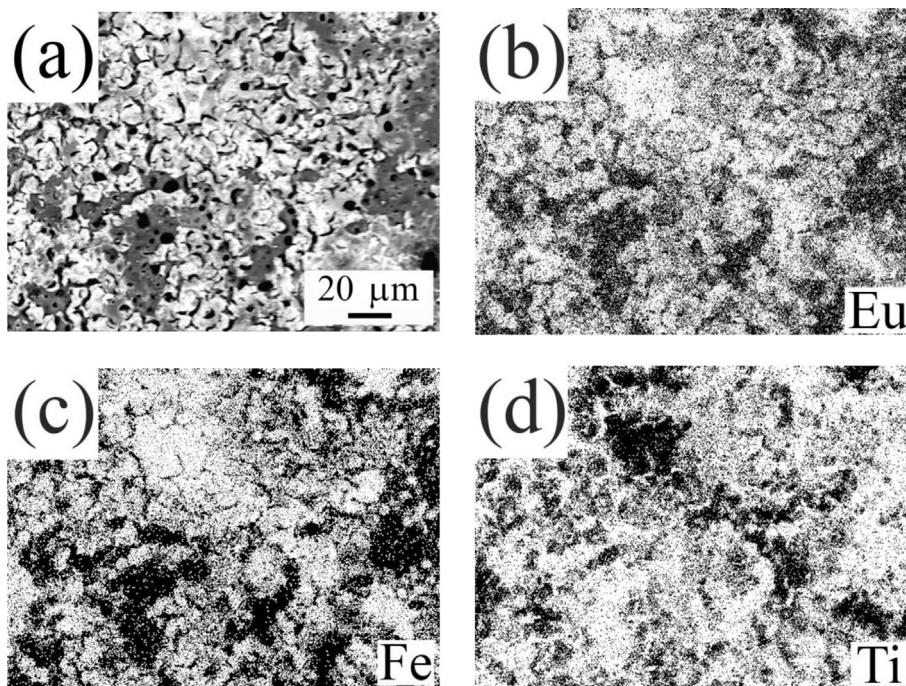


Fig. 2. SEM image (phase representation, a) of the surface of PEO coating after fivefold extract deposition with subsequent annealing and distribution maps (white dots) of europium (b), iron (c), and titanium (d) over the surface.

Table 1
Averaged element composition of the coatings outer layer as to XSA.

Coating	Element composition, at.%						
	O	Na	P	Ti	Fe	Eu	W
PEO	72.2	1.0	4.4	21.4	–	–	0.9
PEO +3 depositions	69.9	–	5.8	18.8	1.8	2.9	0.8
PEO +5 depositions	70.4	–	5.3	15.9	3.5	4.1	0.7

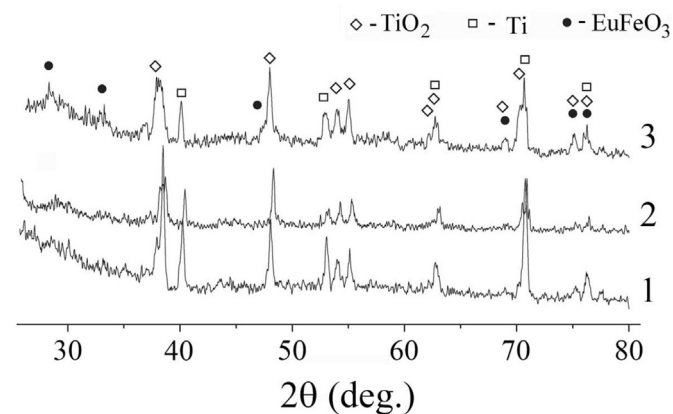


Fig. 3. XRD patterns of titanium samples with PEO coatings before (1) and after threefold (2) and fivefold (3) extract deposition.

The element compositions of the outer layers of initial and modified PEO coatings determined using XSA and averaged over the surface are shown in Table 1. The average values in this Table were obtained for five $300 \times 300 \mu\text{m}$ areas randomly selected over the surface at an analysis depth of 2–5 μm . The main elements

constituting the surface of the PEO coating are oxygen, phosphorus, titanium, and tungsten. The modified PEO coatings contain, in addition, europium and iron, whereas the europium/iron atomic ratio is $\text{Eu/Fe} = 1.6$ (threefold deposition) or $\text{Eu/Fe} = 1.2$ (fivefold deposition). Taking into account the accuracy of the elements determination by the microprobe analysis method (~15%) and the fact that the analysis includes not only the deposited layer, but also the initial PEO coating (with its outer areas as well), one can conclude that the obtained values of the Eu/Fe ratio corroborate a possible presence of EuFeO_3 in the deposited layers.

Fig. 3 shows XRD patterns of the coatings under study. The initial coating (1) contains only the crystalline phase of titanium oxide. Upon modification (2, 3), one observes the emergence of additional reflections corresponding to EuFeO_3 .

The presence of EuFeO_3 is confirmed by XRD, obtaining EuFeO_3 powder by using the same procedure of extraction-pyrolytic synthesis [11], the XSA data indication that the Eu/Fe atomic ratio is approaching 1.0, and localization of Eu and Fe in the same surface areas. However, one cannot exclude the possibility of formation of other oxygen-containing compounds of europium, iron, and titanium in addition to with EuFeO_3 , for example, in the form of solid solutions.

3.2. The features of the deposited layer composition and structure

Upon the extract threefold deposition and annealing, coatings were studied using high-resolution SEM and EDXA (Fig. 4, Table 2). Fig. 4a shows the surface fragment, whose area is comparable with that examined by XSA (Fig. 1cd). This fragment must contain partly areas of both the deposited layer and the initial PEO coating. The latter is also indicated by similarity of the element composition determined by scanning relatively large surface areas on JXA 8100 (Japan) with an INCA Spectrometer (United Kingdom) and Hitachi S5500 (Japan) devices.

During the microprobe analysis (XSA), carbon was excluded from the data (Table 1), since it was preliminarily sputtered on the

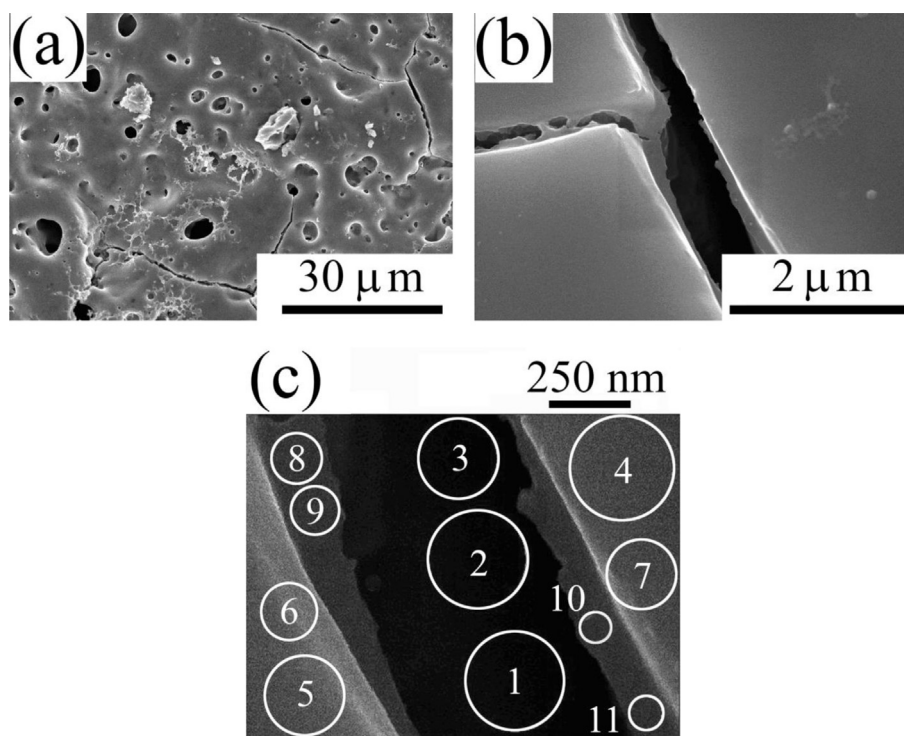


Fig. 4. SEM images of high resolution (a, b, c) of the surface of PEO coating after threefold extract deposition and annealing. Digits indicate areas inside pores (1–3), on the surface of the deposited extract (4–7), and on the pore walls as jutting ‘steps’ (8–11), for which the element composition was determined. The averaged element composition is shown in Table 2.

Table 2

Element composition of the surface, bottom and walls of the pores of the PEO coatings after threefold extract deposition and annealing according to EDXA.

Element	Averaged over area, Fig. 4a	Fig. 4, averaging for areas		
		1, 2, 3	8, 9, 10, 11	4, 5, 6, 7
C	7.4	–	–	6.9
O	61.8	–	12.6	31.1
P	6.0	2.6	5.3	7.3
Ti	22.4	75.8	59.6	46.3
Fe	0.5	13.5	11.3	3.3
Eu	1.1	7.9	10.6	4.2
W	0.8	0.2	0.6	0.9

samples to eliminate the effect of electric charge induction on the analyzed surface. That is why gold was sputtered on the surface to eliminate the above effect during the samples preparations prior to electron microscopy studies and EDXA (Table 2).

The deposited layer areas can be located around cracks present on the surface. The cracks emergence can be caused by compression of the extract layer due to its condensation on less compressible base during the high-temperature annealing. The latter is corroborated by the data of EDXA of the coating material around cracks (Fig. 4c, Table 2). In these sites, the contents of europium and iron are higher than in average over the coating surface. The deposited layer is dense and homogeneous; under the applied magnifications, no individual nanosized particles were found in its composition (Fig. 4bc).

To estimate the chemical composition of the deposited layer over its thickness using an energy dispersive accessory to the microscope, the data on the element composition of the cracks bottom and slopes (on jutting ‘steps’) and the surface around the cracks were obtained (Fig. 4c). Note that the revealed regularities in the composition changes are similar for a few cracks located in

different parts of the deposited layer. The element analysis was carried out on areas limited by circles (Fig. 4c). The obtained data are summarized in Table 2. On the crack bottom, one detected the presence of titanium, iron, europium, phosphorus, and tungsten, while oxygen was not found. The presence of oxygen and the decrease of the titanium concentration were observed on the jutting ‘steps’ in addition to the elements listed above. Finally, the experiment demonstrates the increase of the oxygen concentration on the surface near the crack and the respective decrease of the concentrations of titanium, europium, and iron. Thus, according to experimental data obtained the oxygen content gradually increases from the crack bottom to the deposited layer surface, whereas the titanium concentration, in opposite, decreases in this direction.

The low oxygen concentrations defined at the bottom and steps of the cracks may be associated with the singularities of energy dispersive X-ray analysis in narrow pores. At the same time we cannot exclude that part of the metals in the crack depth may be in a partially reduced state due to the limited penetration of oxygen. In our case, the pyrolysis of used organic extracts containing phenanthroline, tri-*n*-octylamine, acetylacetonate as ligands leads to the formation of volatile reducing agents such as NH₃, CO, H₂, and light hydrocarbons. In the conditions of limited oxygen access, these agents can promote the reducing some metals. For example, as to thermodynamic calculations [26] reducing Fe⁺³ to Fe⁰ may be possible at an annealing temperature of 600 °C in the presence of CO. On the other hand, it is known that in TiO₂/Ti systems fabricated by PEO the diffusion of titanium from the substrate through the pores to the TiO₂ coating surface is observed at temperatures of 800–900 °C [27]. Furthermore, reducing Eu(III) to Eu(II) occurs as a result of Eu(III) organic compounds decomposition in N₂ atmosphere at temperatures of 260–330 °C [28]. To establish the oxidation level and distribution of elements in the cross-section of the coating formed, the additional investigations are required.

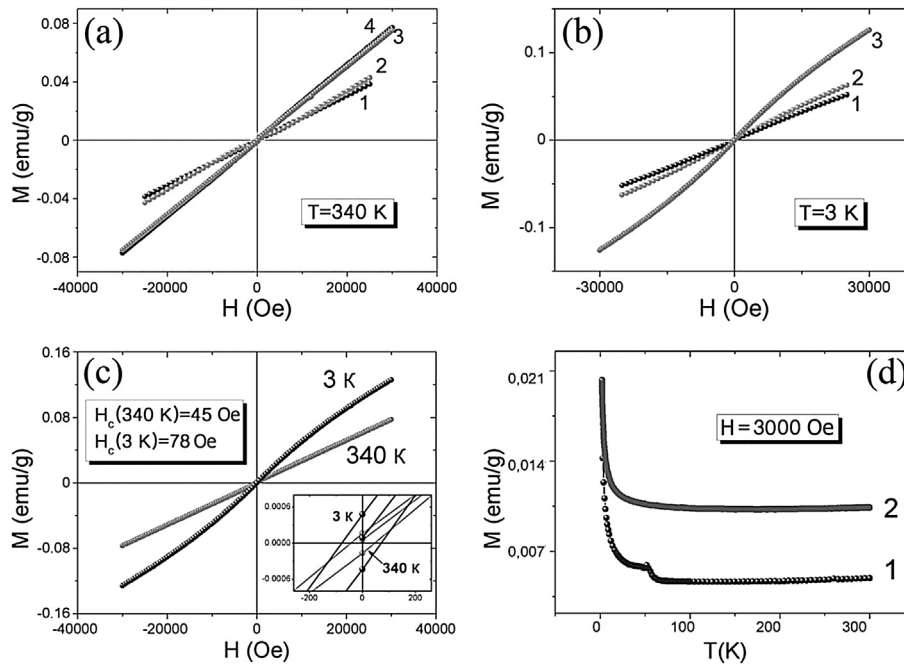


Fig. 5. $M = f(H)$ dependencies (a, b): 1 – titanium; 2 – titanium with PEO coating; 3, 4 – $\text{EuFeO}_3/\text{TiO}_2/\text{Ti}$ composites with threefold and fivefold extract deposition with subsequent annealing. $M = f(H)$ dependencies for the samples with threefold extract deposition at 340 and 3 K (c), insert – the low-intensity field area. Temperature dependencies of the specific magnetization of $\text{EuFeO}_3/\text{TiO}_2/\text{Ti}$ composites in the field $H = 3000$ Oe (d): $M = f(T)$ dependencies 1 and 2 correspond to composites with threefold and fivefold extract deposition.

As can be concluded on the basis of the obtained data, the composition of the deposited layer will be affected by the annealing duration and temperature. In the course of increase of these parameters, the concentration of the oxidized compounds must increase as well.

3.3. Magnetic properties of $\text{EuFeO}_3/\text{TiO}_2/\text{Ti}$ composites

Fig. 5 shows magnetization curves of the initial titanium samples and ‘PEO coating/Ti’ and ‘ $\text{EuFeO}_3/\text{PEO coating}/\text{Ti}$ ’ composites measured at room temperature and 3 K. Titanium (curve 1, Fig. 5ab) and the sample of titanium with PEO coating (curve 2) are paramagnets. Deposition of europium ferrite on the PEO coating increases the value of magnetic susceptibility (curves 3, 4). Analysis of the magnetization curves for low-intensity fields demonstrates that an additional deposition of EuFeO_3 on the surface imparts samples with weak ferromagnetic properties (Fig. 5c). For instance,

at threefold coatings deposition, the value of coercive force H_c at 340 K is equal to 45 Oe, whereas at fivefold deposition it is equal to 63 Oe. The value of the coercive force determined at 3 K differs insignificantly from that measured at room temperature (Fig. 5c).

As follows from the temperature dependence of the samples magnetization values in the field with $H_c = 3000$ Oe, one can trace the trend of this value increase at temperatures above 200 K (Fig. 5d). Such a behavior of these temperature dependencies could indicate to an antiferromagnetic phase transition with the temperature above 340 K. The contributions to the sample magnetization could be provided as by EuFeO_3 present in coatings as by the reduced iron from the layered coatings bulk. Changes in the layer specific magnetization around ~ 50 K (curve 1, Fig. 5d) upon threefold deposition must be caused by the phase transition of the changed magnetic state of europium ferrite. The effect of the reduced iron already present in the layered coating is possible as well. The absence of magnetization anomalies for layers upon fivefold deposition (curve 2, Fig. 5d) could result from the increased content of europium ferrite and its predominant contribution.

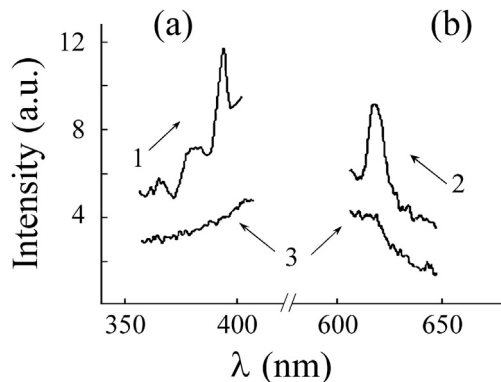


Fig. 6. Luminescence excitation (a) and emission ($\lambda_{\text{ex}} = 395$ nm) spectra (b) of $\text{EuFeO}_3/\text{TiO}_2/\text{Ti}$ (1, 2) composites and TiO_2/Ti (3).

3.4. Luminescent properties of $\text{EuFeO}_3/\text{TiO}_2/\text{Ti}$ composites

Luminescence characteristics of $\text{EuFeO}_3/\text{TiO}_2/\text{Ti}$ composites were estimated from luminescence excitation and emission spectra at 300 K. Fig. 6 shows the luminescence excitation (a) and emission (b) spectra of the composite and the initial TiO_2/Ti substrate. The short-wave range of the luminescence excitation spectrum of the $\text{EuFeO}_3/\text{TiO}_2/\text{Ti}$ composite (curve 1, Fig. 6a) contains, unlike that of the initial TiO_2/Ti substrate, intensive bands ($\lambda_{\text{max}} = 380$ and 400 nm) indicating to the existence of the channel for energy transfer to the Eu^{3+} ion. Simultaneously, one observes the emergence of a number of broad bands ($\lambda_{\text{max}} = 360\text{--}380$ nm) in the luminescence excitation spectrum. This could be caused by the presence of Fe (III) in the samples and/or be the effect of Eu^{3+} ion intraconfiguration $f\text{--}f$ transitions. In the luminescence emission

spectrum of the $\text{EuFeO}_3/\text{TiO}_2/\text{Ti}$ composite (curve 2, Fig. 6b), one registers a luminescence band with the maximum $\lambda_{\text{max}} \approx 620$ nm corresponding to the ${}^5\text{D}_0 - {}^7\text{F}_2$ transition, which is characteristic of the Eu^{3+} ion. Note that the luminescence intensity and the character of the luminescence spectra of the $\text{EuFeO}_3/\text{TiO}_2/\text{Ti}$ composites fabricated at different annealing temperatures in the range 600–970 K and different numbers of deposition cycles did not undergo any changes.

4. Discussion

Layered coatings containing europium ferrite have been fabricated on the surface of TiO_2 oxide through combination of the methods of extraction–pyrolysis synthesis and plasma electrolytic oxidation. Depending on the modification conditions and temperature, the coercive force of the fabricated composites was in the range 45–78 Oe. At 3 K, the coercive force value was about 2 times larger than that at 340 K. The dependence of the composite magnetization on temperature differs from that of free powders of europium ferrite obtained earlier using the extraction–pyrolysis method according to similar scheme [11] and consisting of nanoparticles of a size of 10–20 nm. In the latter case, at temperatures below ~230 K the powders manifested weak ferromagnetic properties, whereas at higher temperatures their ferromagnetism increased dramatically. For instance, at $T = 300$ K, the measured value of the coercive force was equal to 2068 Oe [11]. The fabricated layered metal–oxide composites with europium ferrite on the surface manifest weak ferromagnetic properties in the temperature range 3–340 K. One observes the trend to the increase of the value of specific magnetization at temperatures above 200 K (Fig. 5d). The difference in temperature dependencies of the specific magnetization of nanosized powder of europium ferrite and EuFeO_3 deposited on PEO coating consisting predominantly of TiO_2 must be caused by size effects. The EuFeO_3 properties could be also affected by the substrate and a complex structure of the deposited and annealed layer, due to the presence of a small amount of reduced iron in its composition.

As was shown earlier, in bulk multiferroic samples (for instance, BiFeO_3), observation of the magnetoelectric effect was impossible [2,3,6]. The reason consists in the presence of space–modulated spin structure of the cycloid type in bulk samples [2,3,6]. The magnetoelectric effect can be consistently observed for nanosized samples (example – BiFeO_3 films of a size of dozens and hundreds of nanometers deposited on inert substrates). Destruction of the spin cycloid can be caused not only by the size factor, but also by substitution of bismuth ions with those of rare earth elements [6]. It has been established that polycrystalline samples $\text{R}_x\text{Bi}_{1-x}\text{FeO}_3$, where $\text{R} = \text{Nd}, \text{La}$ or La, Gd , $x = 0.05\text{--}0.2$, fabricated on the basis of BiFeO_3 according to the standard ceramic technology manifest, unlike pure bulk antiferromagnetic bismuth ferrite, weak ferromagnetic properties. Similar features were revealed in the present work for europium ferrite deposited on the titanium oxide substrate. The available literature data and the obtained results enable one to conclude that bulk $\text{EuFeO}_3/\text{TiO}_2/\text{Ti}$ composites fabricated through combination of the methods of plasma electrolytic oxidation and extraction–pyrolysis can be investigated for the presence of magnetoelectric effect in a broad temperature range. Besides, the fabricated composites manifest luminescent properties characteristic of inorganic materials with europium ions.

5. Conclusions

1. The combination of extraction–pyrolysis and plasma electrolytic oxidation may be used for obtaining $\text{EuFeO}_3/\text{TiO}_2/\text{Ti}$

composites simultaneously manifesting luminescent and weak ferromagnetic properties.

2. The energy dispersive X-ray analysis results assume that the deposited layer containing EuFeO_3 can have a complex structure: both oxidized and reduced elements may be present in its composition. For more accurate information about the cross-sectional structure of the combined coating under study, the additional investigations are required.
3. The magnetic properties of EuFeO_3 deposited on PEO coating on titanium are different from those of nanosized powder obtained in Ref. [11]. The $\text{EuFeO}_3/\text{TiO}_2/\text{Ti}$ composite is a weak ferromagnetic through the range of temperatures tested (3–340 K), whereas the ferromagnetism of the powder increases dramatically at temperatures above 230 K.
4. The magnetic properties of deposited EuFeO_3 could be affected by both the metal substrate nature and the complex structure of the deposited and annealed layer.
5. The luminescent properties of $\text{EuFeO}_3/\text{TiO}_2/\text{Ti}$ composites are typical of inorganic materials with europium ions.

Acknowledgments

The authors are grateful to Cand. Sci. (Chem.) V.G. Kuryavyi and Cand. Sci. (Chem.) T.A. Kaidalova for the assistance in determination of the coatings element and phase compositions and morphology.

The study was partially supported by grants no. 15-03-03271 from Russian Foundation for Basic Research and no. 15-1-3-034 from Presidium of FEB RAS.

References

- [1] G.A. Smolenskii, I.E. Chupis, *Segnetomagnetism*, Usp. Fiz. Nauk 137 (3) (1982) 415–448 (in Russian).
- [2] A.P. Pyatakov, A.K. Zvezdin, *Magnetoelectric and multiferroic media*, Phys. Usp. 55 (6) (2012) 557–581.
- [3] G.P. Strokhan, Nanostructured bismuth ferrite films fabricated in transverse RF discharge, *Nanotech. Russ.* 4 (1–2) (2009) 79–84.
- [4] D.I. Khomskii, *Multiferroics: different ways to combine magnetism and ferroelectricity*, J. Magn. Magn. Mater. 306 (1) (2006) 1–8.
- [5] H. Wu, L. Li, L.Z. Liang, S. Liang, Y.Y. Zhu, X.H. Zhu, *Recent progress on the structural characterizations of domain structures in ferroic and multiferroic perovskite oxides: a review*, J. Eur. Ceram. Soc. 35 (2) (2014) 411–441.
- [6] A.F. Ravinski, I.I. Makoev, K.I. Yanushkevich, A.I. Galyas, O.F. Demidenko, A.V. Poddubrovskaya, V.V. Lozenko, V.V. Moshchalkov, *Magnetic properties of multiferroic synthesized based on BiFeO_3* , Phase Transit. Ordered States New Mater. (9) (2012) 17–21 (in Russian), <http://ptosnm.ru/ru/issue/2012/9/78/publication/738>.
- [7] T. Fakhru, R. Mahbub, N. Chowdhury, Q.D.M. Khosru, A. Sharif, *Structural, dielectric and magnetic properties of Ta-substituted $\text{Bi}_{0.8}\text{La}_{0.2}\text{FeO}_3$ multiferroics*, J. Alloy. Compd. 622 (2015) 471–476.
- [8] S.H. Song, Q.S. Zhu, L.Q. Weng, V.R. Mudinepalli, *A comparative study of dielectric, ferroelectric and magnetic properties of BiFeO_3 multiferroic ceramics synthesized by conventional and spark plasma sintering techniques*, J. Eur. Ceram. Soc. 35 (1) (2015) 131–138.
- [9] D. Sando, A. Barthelemy, M. Bibes, *BiFeO_3 epitaxial thin films and devices: past, present and future*, J. Phys. Condes. Matter 26 (47) (2014) 473201.
- [10] M. Mizumaki, T. Uozumi, A. Agui, N. Kawamura, M. Nakazawa, *Admixture of excited states and ground states of a Eu^{3+} ion in $\text{Eu}_3\text{Fe}_2\text{O}_{12}$ by means of magnetic circular dichroism*, Phys. Rev. B 71 (13) (2005) 134416.
- [11] N.I. Steblevskaya, M.A. Medkov, M.V. Belobeletskaya, I.A. Tkachenko, *Europium oxide-based nanocomposites synthesized by extraction–pyrolytic method*, Russ. J. Inorg. Chem. 59 (3) (2014) 251–254.
- [12] A.K. Choquette, R. Colby, E.J. Moon, C.M. Schlepütz, M.D. Scafetta, D.J. Keavney, S.J. May, *Synthesis, structure, and spectroscopy of epitaxial EuFeO_3 thin films*, Cryst. Growth Des. 15 (2015) 1105–1111.
- [13] P. Ciambelli, S. Cimino, S. De Rossi, L. Lisi, G. Minelli, P. Porta, G. Russo, *AFeO_3 ($\text{A} = \text{La}, \text{Nd}, \text{Sm}$) and $\text{LaFe}_{1-x}\text{Mg}_x\text{O}_3$ perovskites as methane combustion and CO oxidation catalysts: structural, redox and catalytic properties*, Appl. Catal. B Environ. 29 (4) (2001) 239–250.
- [14] A.I. Kholkin, T.N. Patrusheva, *Extraction–Pyrolysis Method. Fabrication of Functional Oxide Materials*, KomKniga, Moscow, 2006 (in Russian).
- [15] V.S. Rudnev, M.A. Medkov, N.I. Steblevskaya, I.V. Lukiyanchuk, L.M. Tyrina, M.V. Belobeletskaya, *Pt/SiO₂ and Pt/TiO₂/Ti compositions and their catalytic properties*, Theor. Found. Chem. Eng. 45 (4) (2011) 496–499.
- [16] V.S. Rudnev, M.A. Medkov, T.P. Yarovaya, N.I. Steblevskaya, P.M. Nedovzorov,

- M.V. Belobeletskaya, Combination of plasma-electrolytic oxidation and extraction-pyrolytic method for formation of metal oxide layers, *Russ. J. Appl. Chem.* 85 (4) (2012) 621–628.
- [17] A.G. Rakoch, A.V. Dub, A.A. Gladkova, Anodization of Light Alloys at Different Electric Modes. *Plasma Electrolytic Technology*, Staraya Basmanaya, Moscow, 2012, p. 496 (in Russian).
- [18] A.L. Yerokhin, X. Nie, A. Leyland, A. Matthews, S.J. Dowey, Plasma electrolysis for surface engineering, *Surf. Coat. Technol.* 122 (2–3) (1999) 73–93.
- [19] F.C. Walsh, C.T.J. Low, R.J.K. Wood, K.T. Stevens, J. Archer, A.R. Poeton, A. Ryder, Plasma electrolytic oxidation (PEO) for production of anodised coatings on lightweight metal (Al, Mg, Ti) alloys, *Trans. Inst. Metal. Finish.* 87 (3) (2009) 122–135.
- [20] V.F. Zolin, L.G. Koreneva, *Rare Earth Probe in Chemistry and Biology*, Nauka, Moscow, 1980 (in Russian).
- [21] A.A. Petushkov, S.M. Shilov, V.N. Pak, Dimensional features of the luminescence of europium(III) chloride nanoparticles in a porous glass matrix, *Tech. Phys. Lett.* 30 (11) (2004) 894–896.
- [22] R. Ternane, M. Trabelsi-Ayedi, N. Kbir-Arighuib, B. Piriou, Luminescent properties of Eu^{3+} in calcium hydroxyapatite, *J. Lumines* 81 (3) (1999) 165–170.
- [23] G. Gasparotto, S.A.M. Lima, M.R. Davolos, J.A. Varela, E. Longo, M.A. Zaghete, Luminescence properties of Eu^{3+} - and Mg^{2+} -doped LiTaO_3 obtained via the polymeric precursor method, *J. Lumines* 128 (10) (2008) 1606–1610.
- [24] A. Parma, I. Freris, P. Riello, F. Enrichi, D. Cristofori, A. Benedetti, Structural and photoluminescence properties of $\text{ZrO}_2: \text{Eu}^{3+} @ \text{SiO}_2$ nanophosphors as a function of annealing temperature, *J. Lumines* 130 (12) (2010) 2429–2436.
- [25] V.S. Rudnev, T.P. Yarovaya, A.E. Lysenko, P.M. Nedosorov, N.E. Dushina, The influence of the conditions of forming on the characteristics of the oxide protective films on aluminum, *Prot. Met.* 44 (7) (2008) 715–720.
- [26] H.J.T. Ellingham, *Transactions and communications, J. Soc. Chem. Ind. (London)* 63 (5) (1944) 125–160, <http://dx.doi.org/10.1002/jctb.5000630501>.
- [27] M.S. Vasilyeva, V.S. Rudnev, F. Wiedenmann, S. Wybornov, T.P. Yarovaya, X. Jiang, Thermal behavior and catalytic activity in naphthalene destruction of Ce-, Zr- and Mn-containing oxide layers on titanium, *Appl. Surf. Sci.* 258 (2) (2011) 719–726.
- [28] F. Zhao, S. Gao, Pyrolysis of single molecular precursor for monodisperse lanthanide sulfide/oxysulfide nanocrystals, *J. Mater. Chem.* 18 (2008) 949–953.